

1 “This document is the unedited Author’s version of a Submitted Work that was subsequently
2 accepted for publication in *Environmental Science and Technology*, copyright © American
3 Chemical Society after peer review. To access the final edited and published work see
4 <https://pubs.acs.org/doi/full/10.1021/acs.est.8b00771>”

5 **Bilayer infiltration system combines benefits from both coarse** 6 **and fine sands promoting nutrient accumulation in sediments** 7 **and increasing removal rates**

8 N. Perujo,^{a,b,c*} A.M. Romani,^c and X. Sanchez-Vila^{a,b}

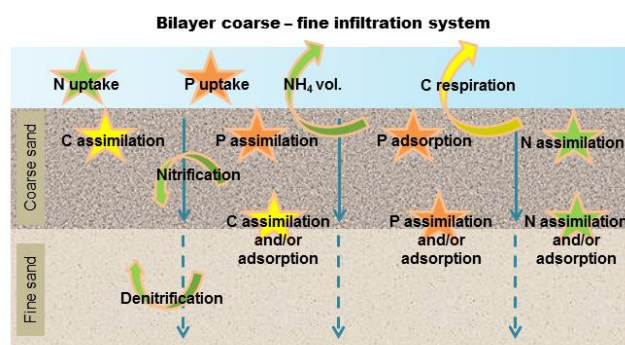
9 ^a Department of Civil and Environmental Engineering, Universitat Politècnica de Catalunya (UPC), Jordi Girona 1-3,
10 08034 Barcelona, Spain

11 ^b Hydrogeology Group (UPC–CSIC), Barcelona, Spain

12 ^c GRECO - Institute of Aquatic Ecology, Universitat de Girona, 17003 Girona, Spain

13 *Corresponding author: nuria.perujo@upc.edu

14 **TOC graphic**



15

16 **Abstract**

17 Infiltration systems are treatment technologies based on water percolation through porous media where
18 biogeochemical processes take place. Grain size distribution (GSD) acts as a driver of these processes and
19 their rates, as well as it influences nutrient accumulation in sediments. Coarse sands inhibit anaerobic
20 reactions such as denitrification and could constrain nutrient accumulation in sediments due to smaller
21 specific surface area. On the other hand, fine sands provide higher nutrient accumulation but need a larger

22 area available to treat the same volume of water; furthermore they are more susceptible to bio-clogging.
23 Combining both sand sizes in a bilayer system would allow infiltrating greater volume of water and the
24 occurrence of aerobic/anaerobic processes. We studied the performance of a bilayer coarse-fine system
25 compared to a monolayer fine one –by triplicate- in an outdoor infiltration experiment to close the C-N-P
26 cycles simultaneously in terms of mass balances. Our results confirm that the bilayer coarse-fine GSD
27 promotes nutrient removal by physical adsorption and biological assimilation in sediments, and further it
28 enhances biogeochemical process rates (two-fold higher than the monolayer system). In overall, the
29 bilayer coarse-fine system allows treating larger volume of water per surface unit achieving similar
30 removal efficiencies as the fine system.

31 **1. Introduction**

32 High nutrient loads into freshwater ecosystems lead worldwide to eutrophication, associated harmful algal
33 blooms, and “dead zones” due to hypoxia (1). In urban areas, the input of nutrients from wastewater
34 treatment plants (WWTP) into freshwaters can contribute to eutrophication processes especially in areas
35 characterized by flow intermittency (2). However, biogeochemical dynamics are affected by numerous
36 factors which hinder the understanding of physical, chemical and biological dynamics related to the
37 potential nutrient removal of water bodies (3). The implementation of infiltration systems in WWTPs
38 before pouring water into streams is considered as a way to decrease nutrient load inputs to rivers, thus
39 diminishing river eutrophication especially during low flow periods (4). Infiltration systems are water
40 treatment technologies that rely on fluid percolation through a porous medium where a combination of
41 biological, chemical, and physical processes help improving the quality of the influent water during the
42 infiltration path (5).

43 The grain size distribution (GSD) of the porous medium is an important characteristic for infiltration
44 systems (6-8). GSD, mostly linked to the pore size distribution and connectivity, modulates the
45 distribution and transport of terminal electron acceptors, nutrients and organic matter in depth (7-8), and
46 acts as a driver of the biogeochemical processes and their rates (9). Also, substrate grain size influences
47 wastewater compounds’ adsorption (10). On one hand, coarse, well-sorted sediments imply large
48 permeability values that result in high dissolved oxygen (DO) concentrations in depth, promoting aerobic
49 processes such as nitrification, but inhibiting anaerobic reactions which are of great importance for the
50 complete total dissolved nitrogen (TDN) removal (11). Furthermore, coarse sediments enhance high loads

51 of nutrients and organic matter which are associated with high biogeochemical rates but with low
52 advection times (12). However, coarse sediments could constrain compounds' adsorption due to smaller
53 specific surface area (13). On the other hand, in fine sediments, the low DO supply through infiltration
54 drives anoxic conditions, where bacteria catalyze full denitrification (14). It is also known that fine sand
55 has larger specific surface area and high adsorbing capacity (15-16) but lower permeability which can
56 constrain wastewater treatment (17) since the risk of substrate clogging may increase (13). Considering
57 all this, it is difficult to assess which substrate size is better to use since both grain sizes display benefits
58 and drawbacks. Accordingly, Perujo et al. (12) carried out an experiment with the aim of deepening in the
59 relationship between physicochemical and biological parameters in different GSDs and results suggested
60 that a bilayer coarse-fine system may integrate the positive aspects of coarse sands and those of fine
61 sands. Kauppinen et al. (18) studied the performance of multi-layered sand filters but focusing mainly on
62 pathogens removal and using combinations of 0-8 mm sand, 0-2 mm biotite and 2-4 mm which showed
63 no different performance between them in terms of nutrients removal. Latrach et al. (19) used a multi-
64 soil-layering system which consisted of a matrix of permeable material (mainly gravel) with soil mixture
65 "boxes" composed of coarse and fine sand, silt and clay, resulting in a high permeable system used to
66 treat raw wastewater, but without carrying out a comparison on amongst system designed with different
67 grain size distributions.

68 The study of biogeochemical processes in sand filters is relatively complex and several processes are
69 involved in the transformation and removal of carbon, nitrogen and phosphorous compounds (20). We are
70 not aware of any work aimed at studying the relevance of a bilayer coarse-fine grain size distribution
71 compared to a monolayer fine sand system to close the C-N-P cycles simultaneously, thus quantifying all
72 the biogeochemical pathways of C, N and P occurring both in the interstitial water and in the sediment
73 surfaces. The main objective of this research is to compare the performance of a bilayer coarse-fine sand
74 system with that of a monolayer fine sand—in triplicate- in an outdoor infiltration experiment and
75 specifically, to study (i) the distribution of biogeochemical processes in the depth profile, (ii) the
76 importance of nutrient accumulation in sediments in regards to adsorption and assimilation processes; and
77 (iii) the link of biogeochemical process rates to removal efficiencies at each system, in order to decipher
78 whether the bilayer system optimizes the performance of infiltration systems. To achieve these objectives,
79 we move away from qualitative process' description, and rely on quantification based on measurements
80 (sampling of interstitial water and sediment and analysis of chemical species in depth from in-situ

81 replicated tanks during 104 days) and validated by means of mass balance evaluations in depth as well as
82 the study of C:N:P molar ratios in sediments to further understand nutrient accumulation processes in
83 sediments.

84 **2. Material and methods**

85 **2.1 Experimental setup**

86 An outdoor infiltration experiment was performed with secondary treated municipal wastewater.
87 Physicochemical parameters of the infiltrated water and nutrient loadings are described in Table S1. Two
88 flow-through sand tank systems (three replicates per system) were created using different GSDs: (1) a
89 bilayer Coarse-Fine (CF) system, consisting of a 20 cm layer of coarse sand (0.9 – 1.2 mm) placed on top
90 of a 20 cm layer of fine sand (0.075 – 0.250 mm); and (2) a monolayer Fine (F) system, with 40 cm of
91 fine sand (0.075 – 0.250 mm) (Fig. S1). Sands were bought from a company dealing (and selling)
92 aggregates (Adicat Tribar, S.L.). They consisted of siliceous sand, rounded shape, free from clays and
93 organic matter and with low metal contents ($\text{Al}_2\text{O}_3 < 0.5 \%$ of the sand dry weight, $\text{Fe}_2\text{O} < 0.04 \%$, $\text{CaO} <$
94 0.05% , and $\text{K}_2\text{O} < 0.5 \%$). Both systems consisted of tanks of 0.21 m^3 capacity and 0.46 m^2 of infiltration
95 surface area; in the upper part of each one, a valve was used to ensure a constant water level creating a
96 constant surface water layer and a continuous infiltration in each system. At the bottom of each tank a
97 gravel layer was placed to facilitate drainage of water towards the outlet to resemble vertical infiltration
98 conditions. There was no water recirculation in the experiment. Three water ports were installed in the
99 wall of the tanks; at depths 4, 18 and 38 cm. The experiment was performed during 104 days from April
100 to July 2016. Outdoor temperature was $21.6 \text{ }^\circ\text{C}$ on average (21) and 234 mm of accumulated rainfall (22)
101 during the time the experiment ran. Sunlight conditions were allowed only in the surface of the tanks, to
102 mimic real infiltration basins. Since the accumulated rainfall only represented 0.12 % and 0.26 % of the
103 daily infiltrated water in our systems (CF and F, respectively) we consider that the effect of rainfall was
104 negligible. Hydraulic parameters of each system as well as organic and nutrient loadings are detailed in
105 Table S1.

106 Water and sediments (note that we use the term “sediment” to refer to the porous media (sand) which is
107 being colonized by biofilm) were sampled weekly at the start and biweekly at the end of the experiment,
108 for a total of 9 sampling campaigns. Samples were collected at about the same time (11 – 12 am), and
109 with consistent weather conditions (sunny, with no registered precipitations two days previous to

110 sampling) to minimize variability due to environmental factors. Water samples were collected from the
111 inlet water, the surface pond, and the three water ports installed at each tank. Dissolved nutrient and
112 organic carbon concentrations were analyzed for all samples.

113 Sediment sampling was performed using a sediment core sampler (Eijkelkamp 04.23.SA) to a depth of 40
114 cm and each core was subdivided in three specific depth layers (0-4 cm as “surface sediment”, 18-22 cm
115 as “20 cm depth sediment” and 36-40 cm as “40 cm depth sediment”). Each sample was homogenized,
116 and then subsamples of 1 cm³ of sediment were collected using an uncapped syringe, and kept frozen (-20
117 °C) until analysis to determine nutrient and carbon content within the sediments. After taking each
118 sediment core, one methacrylate empty column was placed at the same place to avoid the collapse of the
119 surrounding sediment in the tanks, in an attempt to minimize the disruption of the flow field.

120 **2.2 Water analysis**

121 Samples for dissolved nutrients and dissolved organic carbon (DOC) were filtered in pre-combusted (4h,
122 450 °C) filters (GF/F, 0.7 µm, Whatmann). After filtering, dissolved nutrients were analyzed in fresh,
123 while DOC samples were acidified and kept at 4 °C until analysis. DOC concentrations were determined
124 using a total organic carbon analyzer (TOC-V_{CSH} Shimadzu). For inorganic nutrient determination,
125 samples were filtered again (Nylon filters, 0.2 µm, Whatmann) and analyzed as follows: NO_x - as the sum
126 of NO₂⁻ and NO₃⁻ - by ionic chromatography (761 Compact IC 1.1 Metróhm), and NH₄ by the
127 spectrophotometric sodium salicylate protocol (23). Total dissolved nitrogen (TDN) and total dissolved
128 phosphorous (TDP) samples were digested before analysis. The digestion protocol (adapted from
129 Koroleff (24)) consisted in an oxidation where the reagent prepared in NaOH solution (0.375 M)
130 containing K₂S₂O₈ (0.18 M) and H₃BO₃ (0.48 M) was added (2 ml) to filtered samples (20 ml) in tightly
131 capped Pyrex glass tubes. Tubes were closed, shaken and autoclaved (90 min, 115 °C). Absorbance was
132 measured at 275 and 220 nm for TDN determination. TDP determination followed the protocol from
133 Murphy and Riley (25). Dissolved organic nitrogen (DON) was calculated as the difference between TDN
134 and inorganic nitrogen (DON = TDN - (NH₄ + NO_x)).

135 **2.3 Sediment analysis**

136 For carbon and nitrogen determination in sediments, distilled Milli-Q water (1.5 ml) was added to each
137 sediment sample, then sonicated for 1 minute and shook. Aliquots of the extract (100 µl) were pipetted
138 into pre-weight tin cups and placed in the oven at 60 °C until drying. The remaining extract was kept at 4

139 °C. Pipetting was repeated five times to obtain a final dry weight of ca. 1 - 3 mg. Tin cups were weighted
140 and sediment carbon and nitrogen content were analyzed in a CN-analyzer (Carlo Erba).

141 The protocol used for P determination in sediments is adapted from Aspila et al. (26). The samples were
142 dried at 50 °C, crushed and accurately weighted. Samples for total phosphorous (P_{tot}) determination were
143 transferred into porcelain crucibles, ignited in a muffle furnace (550 °C for 1h, following Andersen (27)),
144 and then let to cool for one hour. Samples for total phosphorous and inorganic phosphorous (P_{inorg})
145 determinations were transferred to 100 ml Erlenmeyer flasks with HCl acid (1.0 M, 25 ml). Mixtures
146 were boiled for 15 minutes on a hot plate, filtered (Whatmann, 2.5 μm) to separate the liquid phase from
147 the sediment, and ten-fold diluted with Milli-Q water. P_{tot} and P_{inorg} were determined by the Molybdate-
148 blue method (25). P_{org} was determined by colorimetry, as the difference between P_{tot} and P_{inorg} . The ratio
149 between $P_{\text{inorg}}/P_{\text{org}}$ was calculated as an indicator of the proportion of inorganic phosphorous accumulated
150 in sediments versus the organic phosphorous in sediments, where values >1 indicate dominance of
151 inorganic P and values < 1 indicate dominance organic P. Sediment molar C:N:P ratios were also
152 calculated.

153 **2.4 Removal rates, removal efficiencies and mass balances**

154 **2.4.1 Removal rates**

155 Biogeochemical transformation rates were calculated for different chemical species both in water and
156 sediment. Data were transformed to homogeneous units to allow the comparison between the rates
157 measured in water and in sediment. Total water nutrient loads were calculated at each sampling depth
158 (surface water layer, 4 cm, 18 cm and 38 cm) for all the duration of the experiment, and balances between
159 each two consecutive sampling points were calculated. The results were divided by the total duration of
160 the experiment (104 days) and by the spatial volume of each layer. Data from the sediments were
161 calculated separately for each depth (surface, 20 cm, and 40 cm), multiplied by the conversion factor
162 (1.45 g DW-Dry Weight- per cm^3) and divided by 104 days. All values are reported in $\mu\text{g}\cdot\text{cm}^{-3}\cdot\text{day}^{-1}$.
163 Negative rates indicate a removal process.

164 **2.4.2 Removal efficiencies**

165 Removal efficiencies were calculated from the nutrient loads following equation 1. Two calculations were
166 performed: 1) from the inlet to the outlet, and 2) from the surface of the sediment to the outlet, this one to

167 exclude processes occurring in the layer of surface water and to focus on the processes occurring in the
168 sediment.

$$169 \quad \text{Removal efficiency (\%)} = 100 \cdot (\text{inlet-outlet})/\text{inlet}, \quad (1)$$

170 where, inlet – outlet are the nutrient loads (expressed in $\text{mg} \cdot \text{day}^{-1}$).

171 **2.4.3 Mass balances**

172 Mass balances were calculated from the removal rates and results are reported for different depth
173 infiltration layers (see Figure S1): top layer (includes water mass balance from surface water to 4 cm
174 depth and the C-N-P contents measured in the surface sediment); mid layer (includes water mass balance
175 from 4 cm to 18 cm depth and the sediment C-N-P contents measured at 20 cm depth); and finally, the
176 bottom layer (includes water mass balance from 18 to 38 cm depth and the sediment C-N-P contents
177 measured at 40 cm depth). As the potential processes occurring in the layer of surface water include
178 complex biological (photosynthesis, planktonic uptake of nutrients, organic matter transformation) and
179 chemical (photochemical) reactions that were not monitored, mass balances from inlet water to surface
180 water were not assessed.

181 **2.4.3.1 Carbon mass balances**

182 It is assumed that the main DOC removal pathways are depth dependent. In the upper infiltration layer,
183 the main C transformation pathways are C respiration (C_{resp}) and C accumulation in sediments (C_{sed}),
184 and the mass balance can be expressed as:

$$185 \quad C_{\text{DOC inlet}} - C_{\text{sed}} - C_{\text{resp}} = C_{\text{DOC outlet}} \quad (2)$$

186 In depth, for the mid and bottom layers, transformation pathways are related to C used in denitrification
187 (C_{denitr}), aside from respiration and accumulation in sediments (28). Nonetheless, as the two terms C_{resp}
188 and C_{denitr} were not directly measured in the deeper layers, they were considered as a single term, denoted
189 as $C_{\text{resp/denitr}}$, so that the mass balance equation can be written as:

$$190 \quad C_{\text{DOC inlet}} - C_{\text{sed}} - C_{\text{resp/denitr}} = C_{\text{DOC outlet}} \quad (3)$$

191 **2.4.3.2 Nitrogen mass balances**

192 It is assumed that the main nitrogen transformation pathways are depth dependent: (i) TDN removal
193 pathways in the top infiltration layer are driven by NH_4 volatilization (29) and N accumulation in
194 sediments; (ii) in depth TDN removal pathways consist of denitrification to N gas (30) and N

195 accumulation in sediments (31). Furthermore, (iii) DON can be mineralized to NH_4 (32); (iv) in depth
 196 NO_x can be transformed to DON (33). Also, (v) under oxic conditions NH_4 is nitrified to NO_x (32); (vi) in
 197 depth NO_x can be denitrified to N_2 (14) or reduced to NH_4 (34).

198 According to these assumptions, N mass balances are described. TDN mass balances are given by
 199 equation 4 for the top infiltration layer and 5 for the mid and bottom ones. The main N removal paths are
 200 NH_4 volatilization (denoted in the equations as $TDN_{\text{NH}_4 \text{ volat}}$), N being accumulated in sediments ($TDN_{\text{N sed}}$)
 201 sed), and NO_x denitrification ($TDN_{\text{NO}_x \text{ denitr}}$).

$$202 \quad TDN_{inlet} - TDN_{\text{NH}_4 \text{ volat}} - TDN_{\text{N sed}} = TDN_{outlet} \quad (4)$$

$$203 \quad TDN_{inlet} - TDN_{\text{N sed}} - TDN_{\text{NO}_x \text{ denitrification}} = TDN_{outlet} \quad (5)$$

204 Ammonium mass balances are given by equation 6 for the top layer and 7 for the mid and bottom ones.
 205 Positive contributions on NH_4 mass balances are the DON being mineralized to NH_4 (denoted by $\text{NH}_4_{\text{DON mineral}}$)
 206 $mineral$), and the NO_x being reduced to NH_4 ($\text{NH}_4_{\text{NO}_x \text{ reduction}}$). Negative contributions on ammonium mass
 207 balance are the NH_4 that is being transformed to DON ($\text{NH}_4_{\text{DON prod}}$), the one that left the system via
 208 volatilization ($\text{NH}_4_{\text{volat}}$), the one being nitrified to NO_x ($\text{NH}_4_{\text{nitrif}}$), and that accumulated in the sediment
 209 ($\text{NH}_4_{\text{N sed}}$).

$$210 \quad \text{NH}_4_{inlet} + \text{NH}_4_{\text{DON mineral}} - \text{NH}_4_{\text{volat}} - \text{NH}_4_{\text{nitrif}} - \text{NH}_4_{\text{N sed}} = \text{NH}_4_{outlet} \quad (6)$$

$$211 \quad \text{NH}_4_{inlet} + \text{NH}_4_{\text{NO}_x \text{ reduction}} - \text{NH}_4_{\text{DON prod}} - \text{NH}_4_{\text{N sed}} = \text{NH}_4_{outlet} \quad (7)$$

212 In parallel, NO_x mass balances are given by equation 8 for the top infiltration layer (where there is a net
 213 production) and equation 9 for the mid and bottom ones (with a net reduction). Positive contribution on
 214 NO_x mass balances include NH_4 being nitrified to NO_x ($\text{NO}_x_{\text{prod}}$). The negative terms in the mass balance
 215 equations include the NO_x leaving the system via denitrification ($\text{NO}_x_{\text{denitr}}$), that transformed to NH_4 via
 216 reduction ($\text{NO}_x_{\text{reduction}}$ -in the text called DNRA-), and the NO_x being transformed to DON ($\text{NO}_x_{\text{DON prod}}$).

$$217 \quad \text{NO}_x_{inlet} + \text{NO}_x_{\text{prod}} = \text{NO}_x_{outlet} \quad (8)$$

$$218 \quad \text{NO}_x_{inlet} - \text{NO}_x_{\text{denitr}} - \text{NO}_x_{\text{reduction}} - \text{NO}_x_{\text{DON prod}} = \text{NO}_x_{outlet} \quad (9)$$

219 **2.4.3.3 Phosphorous mass balances**

220 For the phosphorus mass balances, the assumption is that the TDP removal pathways at any depth are
 221 driven by phosphorous content in sediments, $TDP_{\text{P sed}}$ (6). Thus, the TDP mass balance equation is
 222 written as follows:

223
$$TDP_{inlet} - TDP_{P_{sed}} = TDP_{outlet} \quad (10)$$

224 Where $TDP_{P_{sediment}}$ can be also expressed as the sum of phosphorous adsorption in sediments, $TDP_{P_{inorg}}$
225 and phosphorous assimilation, $TDP_{P_{org}}$, resulting in the following mass balance equation:

226
$$TDP_{inlet} - TDP_{P_{inorg}} - TDP_{P_{org}} = TDP_{outlet} \quad (11)$$

227 **2.5 Data Analysis**

228 Dissolved nutrient concentrations and DO were analyzed by repeated measures ANOVA (factors: depth
229 and system, $p < 0.05$). Data for each system were further analyzed separately through Tukey post-hoc
230 analysis to detect significant different groups in depth. The parameters measured in sediments (C, N and
231 P) were analyzed by covariance ANCOVA (factors: depth and system, $p < 0.05$) and further analyzed
232 using the Bonferroni post-hoc test to detect significant different groups in depth and significant
233 differences between systems at each depth. P_{inorg}/P_{org} ratios were also analyzed (ANOVA, factor: depth
234 and system, $p < 0.05$) and the Tukey post-hoc analysis was then applied to all systems separately (factor:
235 depth). Removal rates and removal efficiencies were subject to an ANOVA analysis to detect differences
236 between systems at a given depth and for the overall systems (factor: system, $p < 0.05$). All statistical
237 analyses have been performed using R software (R version 3.1.1, Stats Package).

238 **3. Results**

239 **3.1 Distribution of chemical species in depth**

240 Concentrations of dissolved chemical species measured at each depth are shown in Figures S2 - S5. Both
241 systems showed an increase in DOC, DON and DO concentrations in the surface water layer compared to
242 those in the inlet water. In the surface water layer, there was also a slight decrease in the concentrations of
243 NH_4 , NO_x and TDP for the F system. These slight changes from the inlet water to the surface water layer
244 (although not being statistically significant) resulted in higher NO_x and TDP concentrations in the surface
245 water in the CF system; and higher DO concentration in the F one. A decrease in DOC and DON
246 concentrations was observed in the top sediment layer (surface to 5 cm depth). TDN concentrations
247 gradually decreased in depth, but higher values were measured in CF at 20 cm, as compared to those in F.
248 NH_4 and NO_x concentration profiles in depth were similar in both systems; NH_4 concentration decreased
249 at 5 cm depth but then increased. Oppositely, NO_x concentration increased at 5 cm depth but then
250 decreased. The F system displayed higher NH_4 and lower NO_x concentrations at 20 cm depth, as

251 compared to CF. Both systems displayed a similar pattern for the TDP concentration profile, with a
252 decrease from the surface to 5 cm depth and then stabilization. Higher TDP concentrations were reported
253 in the CF system in the surface and at 20 and 40 cm depth than in the F system. DO concentrations
254 decreased with depth, with lowest values found in the F system at 20 and 40 cm depth.

255 C, N and P concentrations in sediments (Figure 1) were higher in the surface than in the deep layers. The
256 CF system showed higher inorganic P concentration in the surface sediment than F, while for total
257 phosphorous no significant differences between systems were detected. At depths 20 and 40 cm, C, N,
258 inorganic P and total P concentrations in sediments were significantly higher in the CF system than in F.
259 The ratio $P_{\text{inorg}}/P_{\text{org}}$ (Table S2) decreased significantly in depth indicating higher accumulation of organic
260 P than inorganic P in deeper sediments in both systems. In the surface, the CF system showed
261 significantly higher $P_{\text{inorg}}/P_{\text{org}}$ ratio than the F one. Sediment molar ratios are described as follows, in the
262 top layer both systems showed similar C:N ratio ($\approx 7.8 - 7.6$), N: P_{org} ratio ($\approx 14.7 - 17.7$), and C: P_{org} ratio
263 ($\approx 115 - 146$). In the mid layer, C:N ratio increased slightly in both systems ($\approx 8.3 - 9$), and N: P_{org} ratio
264 decreased ($\approx 4.2 - 3.1$) as well as C: P_{org} ratio ($\approx 35.8 - 22.7$). Molar ratios in the bottom layer are similar
265 than in the mid layer, C:N ratio ($\approx 10.2 - 9.0$), N: P_{org} ratio ($\approx 2.7 - 4.3$) and C: P_{org} ratio ($\approx 23.8 - 32.5$ in
266 CF and F, respectively).

267 **3.2 Carbon, nitrogen and phosphorus mass balances**

268 **3.2.1 Carbon mass balances**

269 Carbon mass balances per unit volume of sediment at each sediment layer are described in Figure 2.
270 Removal rates decreased in depth in both systems. In the top layer, DOC removal and C respiration rates
271 were largest in CF while C accumulation rates in sediments were similar between GSDs. This resulted in
272 C accumulation in sediments accounting for 25.1 % and 50.3 % of the DOC removal in CF and F,
273 respectively. Thus, respiration resulted in the main C removal path in the CF system (74.9 %), while in
274 the F one an equal contribution of C accumulation and C respiration to the global DOC balance was
275 found (50.3 % and 49.7 %, respectively). In the middle infiltration layer, both systems were estimated to
276 receive unaccounted C inputs as DOC balances were positive; for this reason, we could not estimate the
277 relative contribution of each carbon removal pathway in that layer, however greatest C accumulation rate
278 in sediments was found in CF. In the bottom layer (20 to 40 cm depth), greatest C accumulation rate was
279 found in CF but similar C respiration rates were described in both systems. In this layer, C_{sed} accounted

280 for 19.1 % and 17.3 %, while $C_{resp/denitr}$ accounted for 80.9 % and 82.7 % of the total DOC removed in
281 the CF and F systems, respectively.

282 **3.2.2 Nitrogen mass balances**

283 Nitrogen mass balances per unit volume of sediment are described in Figure 3. In general, process rates
284 decreased in depth in both systems. In the top infiltration layer, ammonium volatilization was estimated
285 as the main TDN removal path (92.4 % in CF and 90.7 % in F) while N accumulation in the surface
286 sediments accounted for 7.6 % (CF) and 9.3 % (F) of the TDN removal. Notice that only small amounts
287 of N were unaccounted for (3.0 and $0.7 \mu\text{g N}\cdot\text{cm}^{-3}\cdot\text{day}^{-1}$ for CF and F, respectively). In the mid and
288 bottom layers, denitrification was estimated to be the main TDN removal pathway in both systems (90 –
289 95 %) while N accumulation in sediments accounted for only 2 – 10 %. Other N transformation pathways
290 were estimated in the infiltration systems: DON mineralization to NH_4 , and NH_4 nitrification to NO_x in
291 the top infiltration layer; DNRA and NO_x transformation to DON in the middle one, and DNRA in the
292 bottom one.

293 The contributions of these processes in the general balance of intermediate species of N (NH_4 and NO_x)
294 vary between GSDs. Thus, in CF we find that with regard to NH_4 transformation in the upper layer,
295 dominates nitrification (65%). Regarding NO_x transformation in this system, in the middle layer
296 dominates the transformation to DON (43%) and denitrification (55%) and in the lower layer dominates
297 DNRA (72%). However, in the F system, in the top layer dominates both nitrification and ammonium
298 volatilization ($\approx 50\%$ each), in the middle layer dominates DNRA (43%) and denitrification (60%), and in
299 the bottom layer dominates denitrification (80 %). Mass balance closure discrepancies in the mid and
300 bottom layers were very low ($0.17 - 0.25$ and $0.41 - 0.44 \mu\text{g N}\cdot\text{cm}^{-3}\cdot\text{day}^{-1}$ for CF and F, respectively).

301 **3.2.3 Phosphorous mass balances**

302 Mass balances of the P species per unit volume of sediment are described in Figure 4. We assumed that
303 all TDP removed was accumulated in the sediment through adsorption or assimilation. However, in some
304 of the mass balance evaluations, TDP removal was lower than P accumulated in sediments, potentially
305 indicating an unaccounted P input. From Total P accumulated in sediments, proportions between organic
306 and inorganic P were calculated; in surface sediments, results suggested similar accumulation of
307 inorganic P (49 %) and organic P (51 %) in CF, while accumulation of organic P (60 %) contributed more
308 than inorganic P (40 %) in F. At 40 cm depth, organic P accumulation accounted for higher proportion
309 (56 – 63 %) compared to inorganic P (37 – 44 %) in both systems. Higher TDP and P accumulation rates

310 were measured in the top infiltration layer. Comparing systems, TDP removal rate was higher in CF in
311 top and bottom layers and P accumulation rate was higher in the CF system in the mid infiltration layer.

312 **3.3 Removal efficiencies**

313 We report in Table 1 the removal efficiencies of each infiltration system. Considering only the layers that
314 constitute the sediments, both systems showed similar DOC (7 - 11 %), TDN (18 – 23 %) and TDP (14 –
315 16 %) removal efficiencies, but higher TDP and TDN removal rates were reported in CF as compared to
316 F. Including the processes in the full system (three sediment layers plus the surface water layer), the F
317 system resulted in higher TDP removal efficiency (23 %), compared to the CF (12 %).

318 **4. Discussion**

319 Our data support that biogeochemical processes of C-N-P species are depth and GSD dependent, both in
320 qualitative (most relevant processes) and in quantitative terms. As expected, highest rates occurred in the
321 top layer which might be controlled by high nutrient, and DO and electron acceptors availability as well
322 as higher biomass developed in surface sediments compared to deeper ones (35). Regarding our results,
323 nutrient accumulation in the top layer sediments played a key role on nutrient removal efficiencies,
324 especially for DOC and TDP removals (representing up to 50% of their respective removal, while N
325 accumulation in sediment represents 10% of its removal). This removal is suggested to be mainly due to
326 biological processes (assimilation) since the C:N:P elemental molar ratios (calculated from total C and N
327 and organic P in sediments) are close to the known Redfield ratio described for autotrophic biomass
328 (106:16:1, Redfield (36)). Interestingly, even though we expected higher nutrient accumulation rates in
329 the fine sediment due to higher surface area available in fine compared to coarse sediments (37), both
330 systems showed similar rates. Furthermore, in the case of P, where we distinguished the inorganic to the
331 organic fraction, inorganic P showed greater accumulation in the bilayer coarse-fine system. This
332 contradiction could be due to the fact that difference in sediment texture has mostly been associated with
333 the presence of silts and clays (< 2 μm) (38) and in our study the presence of silts and clays was excluded.
334 Furthermore, higher inorganic P accumulation measured in the bilayer system could be related to higher
335 TDP concentrations in the surface water layer (39) which could enhance physical adsorption of inorganic
336 P. It is also worth noting that we are not comparing coarse and fine sands, but GSDs where the bilayer
337 coarse-fine system does not act like coarse homogeneous sediment since physical characteristics such as
338 K and flow velocity are lower than a coarse sediment (12) and therefore both GSDs the bilayer coarse-

339 fine and the monolayer fine systems promote the removal of nutrients through the accumulation of these
340 nutrients in the sediments via adsorption and assimilation.

341 Other significant biogeochemical processes occurring in the top layer of infiltration systems are mostly
342 related to nitrogen (ammonium volatilization and the coupled processes of nitrification and DON
343 mineralization) but also include carbon respiration. As expected, C respiration, nitrification and DON
344 mineralization rates were approximately double in the bilayer system compared to the monolayer system
345 which would indicate that those rates could be proportional to input loads. Greater attention should be
346 focused on ammonium volatilization as it is the main TDN removal pathway in the aerobic top layer of
347 infiltration systems and it seems to be independent of input loads. Ammonium volatilization is a
348 physicochemical process driven by temperatures higher than 20 °C and pH ranging 6.6-8.0 (40) for this
349 reason showed similar rates in both systems.

350 In depth, accumulation of nutrients in sediments was less relevant as a removal path to that observed for
351 the top layer. The slight increase in C:N sediment molar ratios as well as the decrease in C:P_{org} and N:P_{org}
352 ratios compared to the top sediment layer could be linked to the fact that the dominant living biomass in
353 depth is microbial biomass which showed a different elemental molar ratio than autotrophic biomass.
354 Cleveland and Liptzin (41) stated C:N:P = 60:7:1 as the elemental molar ratio for microbial biomass.
355 According to this, sediment molar ratios at 20 and 40 cm depth following the elemental molar ratio
356 described for microbial biomass could be indicative of nutrient assimilation as a main pathway of nutrient
357 accumulation in sediments in depth, but also they could be linked to physical adsorption of microbial
358 biomass that is being transported from upper to lower sediment layers. Specifically, higher accumulation
359 rates in the interface of the bilayer system could be linked to physical entrapment of microbial biomass
360 when reaching the transition from the coarse to the fine sediment layers, as well as retention of carbon,
361 nitrogen and phosphorous species which are then potential to be biologically assimilated or physically
362 adsorbed. At the same time, the imbalance of the molar ratios to a greater accumulation of organic P (low
363 C:P_{org} and N:P_{org} ratios) suggests the deposition of dead organic matter and the accumulation and
364 adsorption of P in lower layers where the mineralization processes of this organic matter could possibly
365 be limited by reduced microbial activity and lower DO. We further contend that unaccounted C inputs
366 reported in the experiment at intermediate depths were probably due to the generation of microbial
367 soluble products (42), or to desorption of organic carbon retained in top sediments (43). Similarly,
368 unaccounted P inputs in mass balances at intermediate depths could be related to the release of

369 phosphates previously assimilated in upper layers by bacteria and algae following their death and
370 subsequent degradation (44).

371 In depth, TDN concentration is the only parameter decreasing in the mid and bottom layers mainly due to
372 anaerobic processes such as denitrification that could take place even in DO concentrations of around 4
373 mg O₂·L⁻¹ (45). Larger loading inputs could explain the larger denitrification rates reported in the bilayer
374 system which resulted in higher TDN removal rates especially in the mid layer as compared to the
375 monolayer fine one. However, sediment GSD in depth modulated N transformation pathways.

376 Specifically, the larger C accumulation in the interface between the coarse and fine layer in CF could
377 favor the conversion of NO_x to DON, most relevant in organic horizons (33). NO_x transformation to
378 DON has been mainly attributed to abiotic processes (46) and specific DON reactions remain unknown.

379 Interestingly, at 40 cm depth, DNRA dominated over denitrification in the CF system, while the opposite
380 happened in the F system. Higher hydraulic conductivity in the former system could have favored
381 interstitial DO transport in depth (11), driving the high DO concentration measured at 20 and 40 cm
382 depth, and being the reason for DNRA being the dominant pathway in depth compared to denitrification
383 (under oxic conditions the denitrification/DNRA ratio is low, Roberts et al. (47)). In this study, different
384 contributions of N transformation pathways between the bilayer and the monolayer systems did not affect
385 the overall TDN removal efficiencies, possibly due to the fact that main differences were achieved in the
386 mid and bottom layers where N concentrations and transformation rates were far smaller than in the top
387 ones.

388 To complete the picture, some comments can be made regarding biogeochemical processes occurring in
389 the surface water layer. Although the observed changes were small, these may have implications in the
390 global nutrient balance in infiltration systems. The most significant changes were the increase in DOC
391 and DON concentrations, related to the potential release of soluble microbial products and algal exudates
392 (48-49), and combined with NH₄, NO_x and TDP concentrations decrease, these associated with possible
393 nutrient uptake by planktonic microorganisms and algae (50-51). Photosynthetic activity in the surface
394 water layer might be responsible for DO concentration increase (52) which, in turn, favours nitrification
395 in the top sediment layer due to high DO concentration in infiltrated water (nitrification has high DO
396 requirements: 4.57 g of O₂ per gram of NH₄, Tchobanoglous (53)).

397 Biogeochemical processes occurring in the surface water layer seem to be directly related to the hydraulic
398 retention time (HRT). This should be interpreted carefully since, as large HRT could favor TDN and TDP
399 removal efficiencies in monolayer fine systems, it could also decrease DOC removal efficiency.

400 Biogeochemical rates - influenced by GSDs - have implications on removal efficiencies in infiltration
401 systems. Main processes related to DOC, TDN and TDP removals are located in the top sediment layer
402 and include C respiration and assimilation, NH₄ volatilization, as well as P assimilation and adsorption.
403 On one hand, the bilayer coarse-fine system allows to infiltrate greater volume of water, and so greater
404 input nutrient loads, than the monolayer fine system. This results in greater rates of biogeochemical
405 processes that are dependent on input loads such as C respiration in the bilayer system. Furthermore, in
406 the bilayer coarse-fine system the convergence of characteristics such as grain size distribution and
407 advection times allows to achieve higher TDN and TDP removal rates in the bilayer, as well as similar or
408 even higher (if comparing values in the interface) nutrient accumulation rates in sediments through
409 physical adsorption and biological assimilation, compared to the monolayer system. Overall, the bilayer
410 coarse-fine system allows to treat a larger volume of water per surface unit achieving similar removal
411 efficiencies as the monolayer fine one.

412 **ACKNOWLEDGEMENTS**

413 We acknowledge support from TRARGISA – Depuradora de Girona, especially to Cristina and Lluís.
414 Also we acknowledge Betty for her support in the lab. This work was supported by the Spanish Ministry
415 of Economy and Competitiveness (GL2014-58760-C3-2-R and project ACWAPUR - PCIN-2015–239),
416 the ERA-NET Cofund Waterworks 2014, the Department of Universitats, Recerca i Societat de la
417 Informació de la Generalitat de Catalunya, and the European Social Fund.

418 **Supporting Information.** Scheme of the two systems used in the experiment; physicochemical
419 parameters measured at the inlet water hydraulic parameters and input loads of each infiltration sand
420 system used; boxplots of dissolved species measured at different depths at each system (DOC, TDN,
421 NO_x, NH₄, DON, TDP and DO) and ratios between inorganic and organic P measured in the sediment.

422 **References**

423 1. Diaz, R. J.; Rosenberg, R. Spreading dead zones and consequences for marine

- 424 ecosystems. *Science* **2008**, 321 (5891), 926-929; DOI 10.1126/science.1156401.
- 425 2. Martí, E.; Riera, J. L.; Sabater, F. Effects of wastewater treatment plants on stream nutrient
426 dynamics under water scarcity conditions. In *Water scarcity in the mediterranean*; Sabater, S.,
427 Barceló, D., Eds.; Springer: Berlin, Heidelberg 2009; pp173-195.
- 428 3. Pai, H.; Villamizar, S. R.; Harmon, T. C. Synoptic Sampling to Determine Distributed
429 Groundwater-Surface Water Nitrate Loading and Removal Potential Along a Lowland
430 River. *Water Resources Research* **2017**, 53 (11), 9479-9495; DOI 10.1002/2017WR020677.
- 431 4. Fox, P. *Soil Aquifer Treatment for sustainable water reuse*; AWWA Research Foundation and
432 American Water Works Association, Denver, CO, 2001.
- 433 5. Dillon, P.; Page, D.; Vanderzalm, J.; Pavelic, P.; Toze, S.; Bekele, E.; Sidhu, J.; Prommer, H.;
434 Higginson, S.; Regel, R.; Rinck-Pfeiffer, S.; Purdie, M.; Pitman, C.; Wintgens, T. A critical
435 evaluation of combined engineered and aquifer treatment systems in water recycling. *Water Sci.*
436 *Technol.* **2008**, 57, 753–762; DOI 10.2166/wst.2008.168.
- 437 6. Brix, H.; Arias, C. A.; del Bubba, M. Media selection for sustainable phosphorus removal in
438 subsurface flow constructed wetlands. *Water Sci. Technol.* **2001**, 44, 47–54.
- 439 7. Boulton, A. J.; Findlay, S.; Marmonier, P.; Stanley, E. H.; Valett, H. M. The Functional
440 Significance of the Hyporheic Zone in Streams and Rivers. *Annu. Rev. Ecol. Syst.* **1998**, 29, 59–
441 81.
- 442 8. Nogaro, G.; Datry, T.; Mermillod-Blondin, F.; Descloux, S.; Montuelle, B. Influence of
443 streambed sediment clogging on microbial processes in the hyporheic zone. *Freshw. Biol.* **2010**,
444 55, 1288–1302; DOI 10.1111/j.1365-2427.2009.02352.x.
- 445 9. Baker, M. A.; Vervier, P. Hydrological variability, organic matter supply and denitrification in
446 the Garonne River ecosystem. *Freshw. Biol.* **2004**, 49, 181–190; DOI 10.1046/j.1365-
447 2426.2003.01175.x.
- 448 10. Ren, Y. X.; Zhang, H.; Wang, C.; Yang, Y. Z.; Qin, Z.; Ma, Y. Effects of the substrate depth on
449 purification performance of a hybrid constructed wetland treating domestic sewage. *J. Environ.*
450 *Sci. Health A* **2011**, 46, 777-782.
- 451 11. Mueller, M.; Pander, J.; Wild, R.; Lueders, T.; Geist, J. The effects of stream substratum texture
452 on interstitial conditions and bacterial biofilms: Methodological strategies. *Limnologica* **2013**,
453 43, 106–113; DOI 10.1016/j.limno.2012.08.002.

- 454 12. Perujo, N.; Sanchez-Vila, X.; Proia, L.; Romaní, A. M. Interaction between Physical
455 Heterogeneity and Microbial Processes in Subsurface Sediments: A Laboratory-Scale Column
456 Experiment. *Environ. Sci. Technol.* **2017**, *51*, 6110–6119; DOI 10.1021/acs.est.6b06506.
- 457 13. Wu, H. M.; Zhang, J.; Ngo, H. H.; Guo, W. S.; Hu, Z.; Liang, S.; Fan, J. L.; Liu, H. A review on
458 the sustainability of constructed wetlands for wastewater treatment: design and operation.
459 *Bioresour. Technol.* **2015**, *175*, 594-601.
- 460 14. Dong, L. F.; Smith, C. J.; Papaspyrou, S.; Stott, A.; Osborn, A. M.; Nedwell, D. B. Changes in
461 Benthic Denitrification, Nitrate Ammonification, and Anammox Process Rates and Nitrate and
462 Nitrite Reductase Gene Abundances along an Estuarine Nutrient Gradient (the Colne Estuary ,
463 United Kingdom). *Appl. Environ. Microbiol.* **2009**, *75*, 3171–3179; DOI 10.1128/AEM.02511-
464 08.
- 465 15. Huang, X.; Liu, C.; Wang, Z.; Gao, C.; Zhu, G.; Liu, L. The Effects of Different Substrates on
466 Ammonium Removal in Constructed Wetlands: A Comparison of Their Physicochemical
467 Characteristics and Ammonium-Oxidizing Prokaryotic Communities. *Clean Soil Air Water*
468 **2013**, *41*, 283–290.
- 469 16. Meng, J.; Yao, Q.; Yu, Z. Particulate phosphorus speciation and phosphate adsorption
470 characteristics associated with sediment grain size. *Ecol. Eng.* **2014**, *70*, 140–145; DOI
471 10.1016/j.ecoleng.2014.05.007.
- 472 17. Zhao, Z.; Chang, J.; Han, W.; Wang, M.; Ma, D.; Du, Y.; Qu, Z.; Chang, S. X.; Ge., Y. Effects
473 of plant diversity and sand particle size on methane emission and nitrogen removal in
474 microcosms of constructed wetlands. *Ecol. Eng.* **2016**, *95*, 390-398.
- 475 18. Kauppinen, A.; Martikainen, K.; Matikka, V.; Veijalainen, A. M.; Pitkänen, T.; Heinonen-
476 Tanski, H.; Miettinen, I. T. Sand filters for removal of microbes and nutrients from wastewater
477 during a one-year pilot study in a cold temperate climate. *J. Environ. Manage.* **2014**, *133*, 206-
478 213.
- 479 19. Latrach, L.; Ouazzani, N.; Masunaga, T.; Hejjaj, A.; Bouhoum, K.; Mahi, M.; Mandi, L.
480 Domestic wastewater disinfection by combined treatment using multi-soil-layering system and
481 sand filters (MSL–SF): A laboratory pilot study. *Ecol. Eng.* **2016**, *91*, 294-301.
- 482 20. Achak, M.; Mandi, L.; Ouazzani, N. Removal of organic pollutants and nutrients from olive mill
483 wastewater by a sand filter. *J. Environ. Manage.* **2009**, *90*(8), 2771-2779.

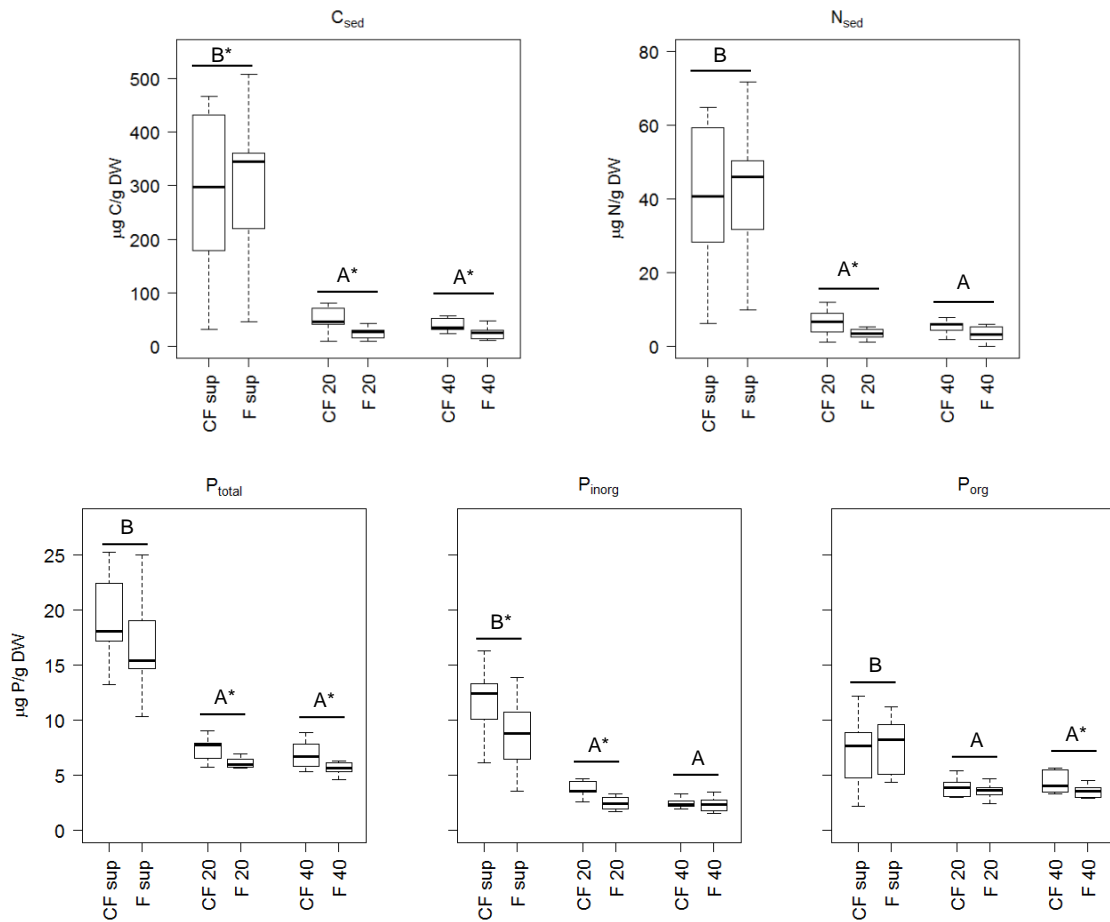
- 484 21. AEMET - State Agency of Meteorology. Ministry of the Environment and Rural and Marine
485 Affairs, Spanish Government. (AEMET - Agencia Estatal de meteorología. Ministerio de Medio
486 Ambiente y Medio Rural y Marino, Gobierno de España) Website;
487 http://www.aemet.es/es/serviciosclimaticos/vigilancia_clima/analisis_estacional (accessed Feb
488 12, 2017).
- 489 22. Meteocat - Meteorological Service of Catalonia. Department of Territory and Sustainability,
490 Government of Catalonia. (Meteocat - Servei meteorològic de Catalunya. Departament de
491 Territori i Sostenibilitat, Generalitat de Catalunya) Website;
492 <http://www.meteo.cat/wpweb/serveis/peticions-de-dades/peticio-dinformes-meteorologics>
493 (accessed Feb 12, 2017).
- 494 23. Reardon, J.; Foreman, J. A.; Searcy, R. L. New reactants for the colorimetric determination of
495 ammonia. *Clin. Chim. Acta* **1966**, 14, 403–405; DOI 0.1016/0009-8981(66)90120-3.
- 496 24. Koroleff, F. Simultaneous oxidation of nitrogen and phosphorus compounds by persulfate.
497 *Methods seawater Anal.* **1983**, 2, 205–206.
- 498 25. Murphy, J.; Riley, J. A modified single solution method for the determination of phosphate in
499 natural waters. *Anal. Chim. Acta* **1962**, 27, 31–36.
- 500 26. Aspila, K.; Agemian, H.; Chau, A. S. A Semi-automated Method for the Determination of
501 Inorganic , Organic and Total Phosphate in Sediments. *Analyst* **1976**, 101, 187–197.
- 502 27. Andersen, J. M. An Ignition Method for Determination of Total Phosphorus in Lake Sediments.
503 *Water Res.* **1976**, 10, 329–331.
- 504 28. Abel, C. D. T.; Sharma, S. K.; Mersha, S. A.; Kennedy, M. D. Influence of intermittent
505 infiltration of primary effluent on removal of suspended solids, bulk organic matter, nitrogen and
506 pathogens indicators in a simulated managed aquifer recharge system. *Ecol. Eng.* **2014**, 64, 100–
507 107; DOI 10.1016/j.ecoleng.2013.12.045.
- 508 29. Reddy, G. B.; Hunt, P. G.; Phillips, R.; Stone, K.; Grubbs, A. Treatment of swine wastewater in
509 marsh-pond-marsh constructed wetlands. *Water Sci. Technol.* **2001**, 44, 545 – 550.
- 510 30. Reddy, K. R.; D’Angelo, E. M. Biogeochemical indicators to evaluate pollutant removal
511 efficiency in constructed wetlands. *Water Sci. Technol.* **1997**, 35, 1–10; DOI 10.1016/S0273-
512 1223(97)00046-2.
- 513 31. Bitton, G. Role of microorganisms in biogeochemical cycles. In *Wastewater microbiology*;

- 514 Bitton, G., Ed.; John Wiley and Sons: New Jersey 1999; pp 75-105.
- 515 32. Ruane, E. M.; Murphy, P. N. C.; French, P.; Healy, M. G. Comparison of a Stratified and a
516 Single-Layer Laboratory Sand Filter to Treat Dairy Soiled Water from a Farm-Scale Woodchip
517 Filter. *Water, Air, Soil Pollut.* **2014**, 225, 1–10; DOI 10.1007/s11270-014-1915-z.
- 518 33. Dail, D.B.; Davidson, E. A.; Chorover, J. Rapid abiotic transformation of nitrate in an acid forest
519 soil. *Biogeochemistry* **2001**, 54, 131–146.
- 520 34. Tiedje, J. M. Ecology of denitrification and dissimilatory nitrate reduction to ammonium. In
521 *Environmental Microbiology of Anaerobes*; Zehnder, A. J. B., Ed.; John Wiley and Sons: New
522 York 1988; pp 179–244.
- 523 35. Freixa, A.; Rubol, S.; Carles-Brangarí, A.; Fernàndez-Garcia, D.; Butturini, A.; Sanchez-Vila,
524 X.; Romání, A. M. The effects of sediment depth and oxygen concentration on the use of organic
525 matter: An experimental study using an infiltration sediment tank. *Sci. Tot. Env.* **2016**, 540, 20-
526 31.
- 527 36. Redfield, A. C. The biological control of chemical factors in the environment. *American scientist*
528 **1958**, 46(3), 230A-221.
- 529 37. Zhu, H.; Wang, D.; Cheng, P.; Fan, J.; Zhong, B. Effects of sediment physical properties on the
530 phosphorus release in aquatic environment. *Science China Physics, Mechanics & Astronomy*
531 **2015**, 58(2), 1-8.
- 532 38. Liu, Q.; Liu, S.; Zhao, H.; Deng, L.; Wang, C.; Zhao, Q.; Dong, S. The phosphorus speciations
533 in the sediments up-and down-stream of cascade dams along the middle Lancang River.
534 *Chemosphere* **2015**, 120, 653-659.
- 535 39. Del Bubba, M.; Arias, C. A.; Brix, H. Phosphorus adsorption maximum of sands for use as
536 media in subsurface flow constructed reed beds as measured by the Langmuir isotherm. *Water*
537 *Res.* **2003**, 37(14), 3390-3400.
- 538 40. Poach, M.; Hunt, P.; Reddy, G.; Stone, K.; Matheny, T.; Johnson, M. H.; Sadler, E. J. Ammonia
539 Volatilization from Marsh-Pond-Marsh Constructed Wetlands. *J. Environ. Qual.* **2004**, 33, 844–
540 851.
- 541 41. Cleveland, C.C.; Liptzin, D. C: N: P stoichiometry in soil: is there a “Redfield ratio” for the
542 microbial biomass? *Biogeochemistry* **2007**, 85(3), 235-252.
- 543 42. Essandoh, H. M. K.; Tizaoui, C.; Mohamed, M. H. A. Removal of dissolved organic carbon and

- 544 nitrogen during simulated soil aquifer treatment. *Water Res.* **2013**, 47, 3559–3572; DOI
545 10.1016/j.watres.2013.04.013.
- 546 43. Quanrud, D. M.; Hafer, J.; Karpiscak, M. M.; Zhang, J.; Lansey, K. E.; Arnold, R. G. Fate of
547 organics during soil-aquifer treatment: sustainability of removals in the field. *Water Res.* **2003**,
548 37, 3401–3411.
- 549 44. Essandoh, H. M. K.; Tizaoui, C.; Mohamed, M. H. A.; Amy, G.; Brdjanovic, D. Soil aquifer
550 treatment of artificial wastewater under saturated conditions. *Water Res.* **2011**, 45, 4211–4226;
551 DOI 10.1016/j.watres.2011.05.017.
- 552 45. Gao, H.; Schreiber, F.; Collins, G.; Jensen, M. M.; Kostka, J. E.; Lavik, G.; de Beer, D.; Zhou,
553 H.; Kuypers, M. M. Aerobic denitrification in permeable Wadden Sea sediments. *ISME J.* **2010**,
554 4, 417–426; DOI 10.1038/ismej.2010.166.
- 555 46. Rückauf, U.; Augustin, J.; Russow, R.; Merbach, W. Nitrate removal from drained and reflooded
556 fen soils affected by soil N transformation processes and plant uptake. *Soil Biol. Biochem.* **2004**,
557 36, 77–90; DOI 10.1016/j.soilbio.2003.08.021.
- 558 47. Roberts, K. L.; Kessler, A. J.; Grace, M. R.; Cook, P. L. M. Increased rates of dissimilatory
559 nitrate reduction to ammonium (DNRA) under oxic conditions in a periodically hypoxic
560 estuary. *Geochim. Cosmochim. Acta* **2014**, 133, 313–324; DOI 10.1016/j.gca.2014.02.042.
- 561 48. Czerwionka, K. Influence of dissolved organic nitrogen on surface waters. *Oceanologia* **2016**,
562 58, 39–45; DOI 10.1016/j.oceano.2015.08.002.
- 563 49. Siczko, A.; Maschek, M.; Peduzzi, P. Algal extracellular release in river-floodplain dissolved
564 organic matter: Response of extracellular enzymatic activity during a post-flood period. *Front.*
565 *Microbiol.* **2015**, 6, 1–15; DOI 10.3389/fmicb.2015.00080.
- 566 50. Hein, M.; Pedersen, M. F.; Sand-Jensen, K. Size-dependent nitrogen uptake in micro- and
567 macroalgae. *Mar. Ecol. Prog. Ser.* **1995**, 118, 247–253.
- 568 51. Kirchman, D. L. The uptake of inorganic nutrients by heterotrophic bacteria. *Microb. Ecol.*
569 **1994**, 28, 255–271; DOI 10.1007/BF00166816.
- 570 52. Drapcho, C. M.; Brune, D. E. The partitioned aquaculture system : impact of design and
571 environmental parameters on algal productivity and photosynthetic oxygen production. *Aquac.*
572 *Eng.* **2000**, 21, 151–168.
- 573 53. Tchobanoglous, G. Fundamentals of biological treatment. In *Wastewater Engineering:*

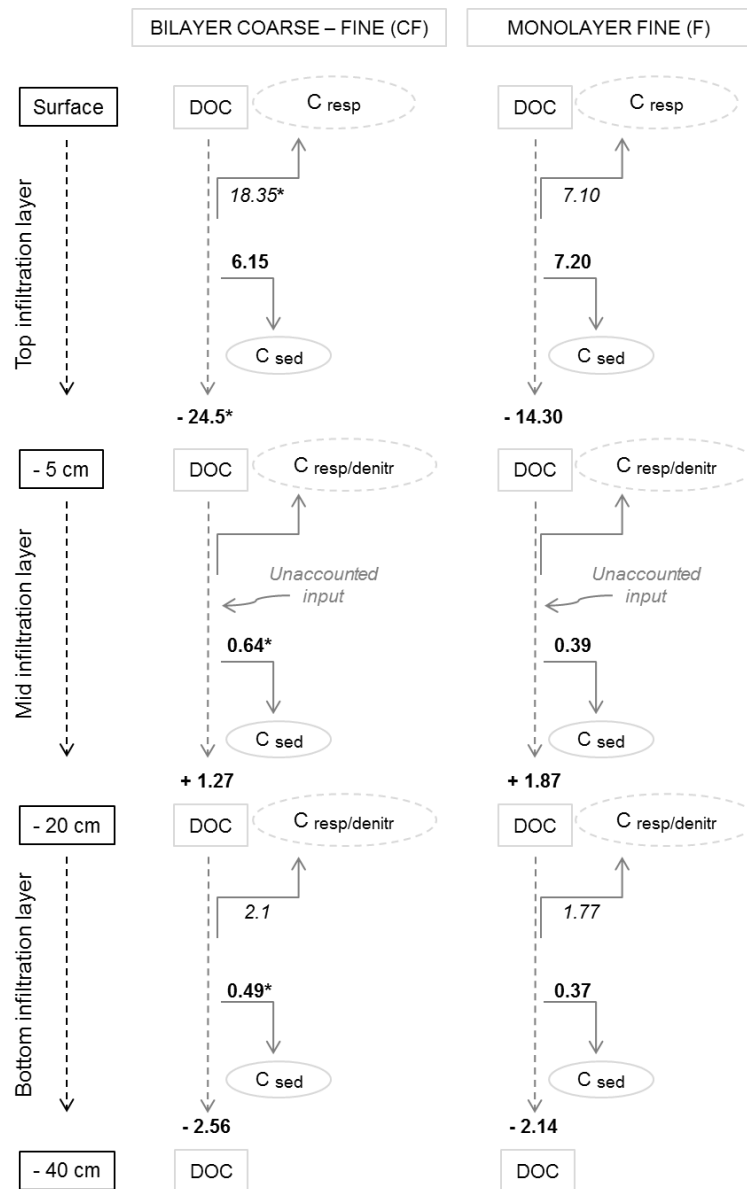
574 *Treatment and Reuse*; Tchobanoglous, G., Burton, F.L., Stensel, H.D., Eds.; Metcalf & Eddy
575 Inc: New York 2003; pp 611–635.
576

577 **Figures**



578 **Figure 1** Boxplots for carbon, nitrogen and phosphorous species (total P, inorganic P and organic P)
 579 concentrations measured in sediments as a function of depth (sup: superficial, 20: 20 cm depth, 40: 40 cm
 580 depth) and GSDs (CF: bilayer coarse-fine system; F: monolayer fine system) and Tukey's post-hoc
 581 analysis after ANCOVA analysis for depth ($p < 0.05$). Asterisks determine differences between GSDs at
 582 each given depth (ANCOVA, $p < 0.05$).

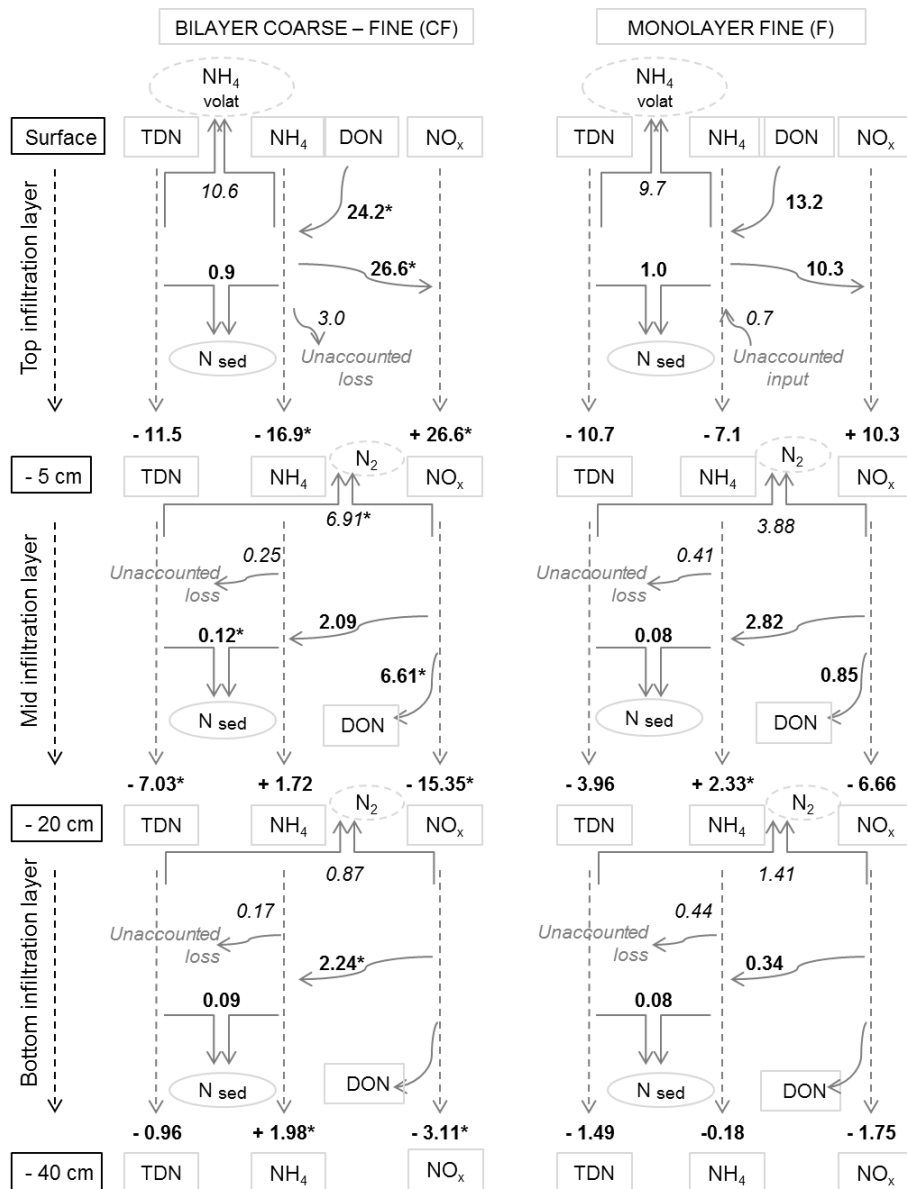
583



584

585 **Figure 2** Carbon mass balances for the main C transformation processes and removal paths in the
 586 sediment layers. Values in **bold** indicate mass balances calculated from experimental data while values in
 587 *italic* are parameters estimated through equations 2 and 3. Asterisk indicates significant difference
 588 between systems (ANOVA, factor: system, $p < 0.05$). Dotted oval circles refer to dissolved species that
 589 leave the system via gas; solid line oval circles refer to dissolved species that are being accumulated in
 590 the sediment. Results are expressed as $\mu\text{g C}\cdot\text{cm}^{-3}\cdot\text{day}^{-1}$. Negative values indicate dissolved components
 591 removal.

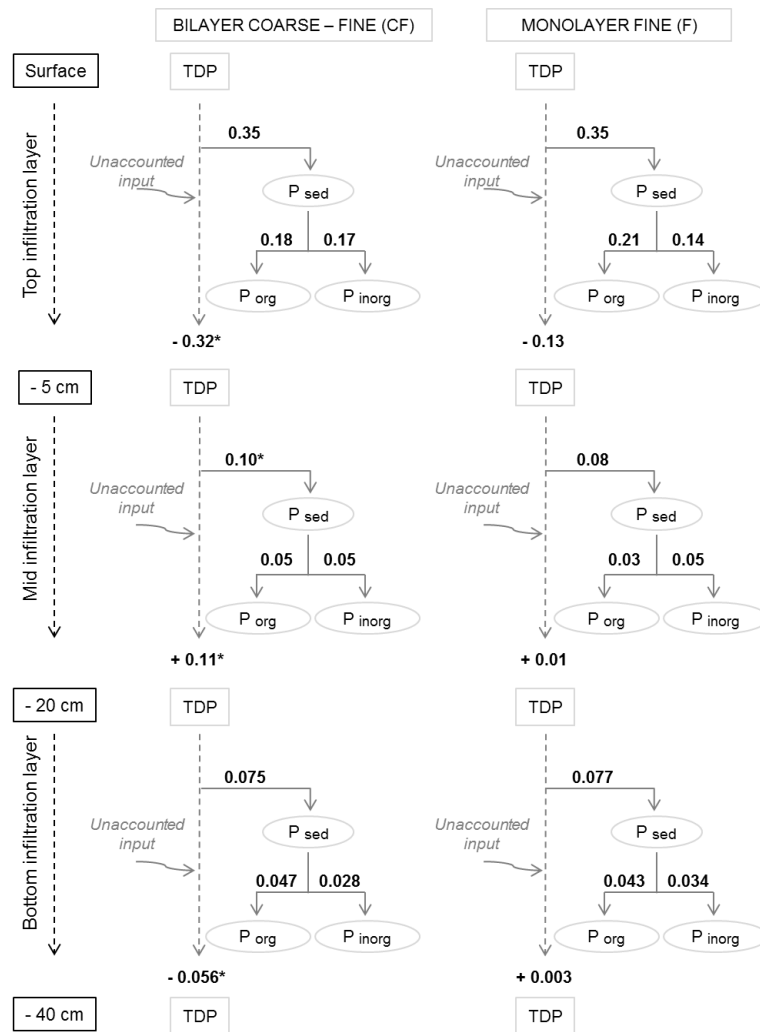
592



593

594 **Figure 3** Nitrogen mass balances for the main N transformation processes and removal paths in the
 595 sediment layers. Values in **bold** indicate mass balances calculated from experimental data while values in
 596 *italic* are parameters estimated through equations 4-9. Asterisk indicates significant difference between
 597 systems (ANOVA, factor: system, $p < 0.05$). Dotted oval circles refer to dissolved species that leave the
 598 system via gas; solid line oval circles refer to dissolved species that are being accumulated in the
 599 sediment. Results are expressed as $\mu\text{g N}\cdot\text{cm}^{-3}\cdot\text{day}^{-1}$. Negative values indicate dissolved components
 600 removal. DON balances in the bottom layer resulted in low and highly uncertain values, and so, they were
 601 excluded from mass balance calculations.

602



603

604 **Figure 4** Phosphorous mass balances for the main P transformation processes and removal paths in the
 605 sediment layers. Values in **bold** indicate mass balances calculated from experimental data while values in
 606 *italic* are parameters estimated through equations 10 and 11. Asterisk indicates significant difference
 607 between systems (ANOVA, factor: system, $p < 0.05$). Solid line oval circles refer to dissolved species that
 608 are being accumulated in the sediment. Results are expressed as $\mu\text{g P} \cdot \text{cm}^{-3} \cdot \text{day}^{-1}$. Negative values indicate
 609 dissolved components removal.

610

611 **Tables**612 **Table 1** Removal efficiencies (%) and overall removal rates measured in the infiltration systems

		Surface – 40 cm depth		Inlet – 40 cm depth	
		CF	F	CF	F
DOC	%	7.44 ± 2.7	11.31 ± 1.8	5.50 ± 4.5	6.53 ± 2.0
	Removal rate	-3.87 ± 1.1	-2.15 ± 0.4		
TDN	%	18.45 ± 3.1	23.03 ± 2.6	17.23 ± 2.7	22.75 ± 4.2
	Removal rate	-4.55 ± 0.5	-3.57 ± 0.2		
TDP	%	13.91 ± 3.0	16.46 ± 5.4	11.87 ± 2.6	25.67 ± 4.3
	Removal rate	-0.027 ± 0.005	-0.011 ± 0.002		

613 Removal rates are expressed as $\mu\text{g C}\cdot\text{cm}^{-3}\cdot\text{day}^{-1}$ for DOC, $\mu\text{g N}\cdot\text{cm}^{-3}\cdot\text{day}^{-1}$ for TDN and $\mu\text{g P}\cdot\text{cm}^{-3}\cdot\text{day}^{-1}$
614 for TDP. Considering only the sediment part of the systems (three infiltration layers) correspond to the
615 column “Surface – 40 cm depth”, while removal efficiencies for the whole system, including the surface
616 water layer correspond to the column “Inlet – 40 cm depth”. Values in bold indicate the system with
617 significant higher value of the specified parameter comparing systems (ANOVA, factor: system, $p <$
618 0.05).